Valence ionized states of iron pentacarbonyl and η^5-cyclopentadienyl cobalt dicarbonyl studied by symmetry-adapted cluster-configuration interaction calculation and collision-energy resolved Penning ionization electron spectroscopy

Ryoichi Fukuda,[1,2,3,a)] Masahiro Ehara,[1,3] Hiroshi Nakatsuji,[2,3] Naoki Kishimoto,[4] and Koichi Ohno[4,5]
[1]*Department of Theoretical and Computational Molecular Science, Institute for Molecular Science and Research Center for Computational Science, 38 Nishigo-Naka, Myodaiji, Okazaki 444-8585, Japan*
[2]*Quantum Chemistry Research Institute, Kyodai Katsura Venture Plaza, 1-36 Goryo Oohara, Nishikyo-ku, Kyoto 615-8245, Japan*
[3]*CREST, Japan Science and Technology Agency, Sanboncho-5, Chiyoda-ku, Tokyo 102-0075, Japan*
[4]*Department of Chemistry, Graduate School of Science, Tohoku University, Aramaki, Aoba-ku, Sendai 980-8578, Japan*
[5]*Toyota Physical and Chemical Research Institute, Nagakute, Aichi 480-1192, Japan*

(Received 9 December 2009; accepted 26 January 2010; published online 23 February 2010)

Valence ionized states of iron pentacarbonyl $Fe(CO)_5$ and η^5-cyclopentadienyl cobalt dicarbonyl $Co(\eta^5\text{-}C_5H_5)(CO)_2$ have been studied by ultraviolet photoelectron spectroscopy, two-dimensional Penning ionization electron spectroscopy (2D-PIES), and symmetry-adapted cluster-configuration interaction calculations. Theory provided reliable assignments for the complex ionization spectra of these molecules, which have metal-carbonyl bonds. Theoretical ionization energies agreed well with experimental observations and the calculated wave functions could explain the relative intensities of PIES spectra. The collision-energy dependence of partial ionization cross sections (CEDPICS) was obtained by 2D-PIES. To interpret these CEDPICS, the interaction potentials between the molecules and a Li atom were examined in several coordinates by calculations. The relation between the slope of the CEDPICS and the electronic structure of the ionized states, such as molecular symmetry and the spatial distribution of ionizing orbitals, was analyzed. In $Fe(CO)_5$, an attractive interaction was obtained for the equatorial CO, while the interaction for the axial CO direction was repulsive. For $Co(\eta^5\text{-}C_5H_5)(CO)_2$, the interaction potential in the direction of both Co–C–O and Co–Cp ring was attractive. These anisotropic interactions and ionizing orbital distributions consistently explain the relative slopes of the CEDPICS. © *2010 American Institute of Physics*. [doi:10.1063/1.3319778]

I. INTRODUCTION

The energy spectrum of valence ionized states of molecules is an intrinsic property that can be directly observed by experimental techniques and contains information on the electronic structure and chemical bonds. Although Koopmans' theorem[1] is useful for theoretical interpretation of these states, it is insufficiently predictive for transition metal compounds because electron correlation and orbital relaxation following ionization are significant. Experimental techniques have been developed for the analysis of ionization bands such as variable energy photoelectron spectroscopy,[2] electron momentum spectroscopy,[3–5] and two-dimensional (2D) Penning ionization electron spectroscopy (PIES)[6–8] to obtain useful information from the spectra. High-level theoretical calculations are mandatory for a reliable enough assignment and analysis of ionization spectra in order to study the detailed interplay of spectra and molecular structure, such as chemical bonds, inductive and ligand field effects, n-conjugation, cyclic strains, molecular conformation, etc.[5,9,10] Theoretical calculations are essential also to analysis of the recent orbital-imaging experiments by ionization spectroscopy.[11,4]

Recently, two of the authors reported the 2D-PIES of a half-sandwich organometallic compound, η^5-cyclopentadienyl cobalt dicarbonyl $[Co(\eta^5\text{-}C_5H_5)(CO)_2]$ with theoretical calculations by the symmetry-adapted cluster-configuration interaction (SAC-CI) and P3 propagator methods.[12] The SAC-CI method[13,14] accurately describes both the electron correlation and orbital relaxation effects, and therefore it is a suitable theory for reliable prediction of ionization energies (IEs) of molecules. Indeed, the SAC-CI method has been successfully applied to the chemistry and spectroscopy of various types of ionized states.[15–17] For the IEs of $CoCp(CO)_2$ ($Cp=C_5H_5$), however, the agreement between the SAC-CI calculations and the experimental results was not sufficient because the computational condition was inadequate. An accurate description of both metal and ligand ionizations requires a high level of computation,[18] but such a calculation was very expensive using our previous SAC-CI program.

We have developed a new algorithm and program for the SAC-CI method, which we designate the direct SAC-CI for

a)Electronic mail: fukuda@ims.ac.jp.

more efficient and accurate calculations.[19] The direct SAC-CI method uses a direct CI-like algorithm that is combined with the perturbation-selection technique.[20] Because of its efficiency, the direct SAC-CI method includes terms that were neglected in the previous version of the nondirect SAC-CI program for reduction in computational labor. In addition, a larger basis set can be employed to improve the reliability of the calculations. Recently, the direct SAC-CI method was applied to the valence ionization of group six metal carbonyls.[21] In that study, the direct SAC-CI calculations provided reliable assignment of spectra and the importance of orbital-reorganization terms that were not sufficiently included in our previous study was confirmed.

In this study, we investigate the valence ionization spectra of iron pentacarbonyl $[Fe(CO)_5]$ and $CoCp(CO)_2$ by He I UV photoelectron spectra (UPS), PIES, and quantum chemical calculation using the direct SAC-CI method. We are particularly interested in the ionization of metal-carbonyl bonds in which various types of orbitals, namely, $CO(\sigma)$, $CO(\pi)$, metal $3d$, $4s$, and $4p$, are involved. They are prototype chemical bonds of organometallic compounds and are also a model for carbon monoxide on metal surfaces;[22] therefore, it is important to develop theoretical and spectroscopic methods to investigate the electronic structures of these types of compounds.

Penning ionization occurs when a target molecule M collides with an excited rare gas atom A^* having an excitation energy larger than the IE of M,[7]

$$A^* + M \rightarrow A + M^+ + e^-. \quad (1)$$

The reaction probability depends on the spatial overlap of an ionizing orbital of M and the inner singly occupied orbital of A^*. Therefore, PIES has been regarded as a sensitive probe for the electron density distribution of ionizing orbitals.[3,23,24] The collision-energy dependence of partial ionization cross sections (CEDPICS),[7,8] which is measured by 2D-PIES,[6–8] relates to anisotropic interactions between A^* and M. The slope of CEDPICS with respect to the collision energy reflects attractive or repulsive interactions between A^* and M along the reaction coordinate.[7,8,23,24]

Several studies have been reported for the valence ionization of $Fe(CO)_5$.[9,24,25] Fundamental assignment of the ionization bands has already been established; however, the agreement between theory and experiment was still not satisfactory and a more detailed interpretation is necessary. The present study has given reliable assignments and interpretation for the ionized states in the outer-valence region below 20 eV. The electronic structure of the Fe–CO bonds has been studied by theoretical calculations and the effect of electron correlation has been discussed. The present calculation has also provided a reasonable interpretation of CEDPICS using the potential energy surfaces and anisotropic character of the molecular surface. We have proposed a relation between the slope of CEDPICS and the shape of the orbitals, in particular, their symmetry.[25]

For the valence ionization spectrum of $CoCp(CO)_2$, many electronic states exist in a narrow energy range and its spectrum is more complicated than those of metal carbonyls or metallocenes; therefore, an accurate theoretical study is necessary to provide reliable assignments. However, a previous variable energy photoelectron study,[26] an $X\alpha$-SW calculation,[26] and a SAC-CI study[12] have not shown sufficient agreement between the theoretical and experimental results; in particular, the assignments of bands higher than 13 eV are still debatable. The present calculation has provided a reliable assignment that is consistent with the UPS and 2D-PIES observations. The present study shows a new research technique for valence electronic structures of molecules using 2D-PIES and high-level *ab initio* calculations to investigate IE levels and spatial distribution of valence electrons.

II. EXPERIMENT

The experimental apparatus used in this study has been reported in previous papers.[8,12] Beams of electronically excited metastable $He^*(2\,^{1,3}S)$ atoms were produced by a nozzle discharge source with a tantalum hollow cathode. The $He^*(2\,^1S)$ component was eliminated by a water-cooled helium discharge lamp (quench lamp), while $He^*(2\,^3S)$ metastable atoms (19.82 eV) were led to the collision cell in the reaction chamber. He I UPS were measured using the He I resonance photons (584 Å, 21.22 eV) produced by a discharge in pure helium gas. The kinetic energy of the ejected electrons was measured by a hemispherical electrostatic deflection-type analyzer using an electron collection angle of 90° relative to the incident $He^*(2\,^3S)$ or photon beam. Measurement of the full width at half-maximum (FWHM) of the $Ar^+(^2P_{3/2})$ peak in the He I UPS led to an estimate of 60 meV for the energy resolution of the electron energy analyzer. The transmission efficiency curve of the electron energy analyzer was determined by comparing our UPS data with transmission-corrected UPS data.[27] The background pressure in the reaction chamber was of the order of 10^{-7} Torr. $Fe(CO)_5$ was introduced to the main chamber by heating the sample tube at 30–40 °C.

In the experimental setup for the 2D Penning ionization electron measurement, the metastable atom beam was modulated by a pseudorandom chopper[28] and then introduced into a reaction cell located 504 mm downstream from the chopper disk. The experimental apparatus for $He^*(2\,^3S)$ 2D-PIES has been reported previously.[6–8] The measured Penning ionization spectra $I_e(E_e,t)$ were stored as a function of the electron kinetic energy (E_e) and time (t). Analysis of the time-dependent Penning ionization spectra by means of the Hadamard transformation and normalization by the velocity distribution of the He^* beam can lead to a 2D mapping of the Penning ionization cross section $[\sigma(E_e,E_c)]$ as a function of the electron energy, E_e, and collision energy, E_c. The velocity distribution in the metastable He^* beam was determined by monitoring secondary electrons emitted from a stainless steel plate inserted in the reaction cell. The resolution of the analyzer was reduced to 250 meV to obtain higher counting rates for the Penning electrons. The slope parameter (m) of the CEDPICS was obtained by a least-squares method in the E_c range from approximately 100 to 300 meV.

III. COMPUTATIONAL DETAILS

The ground and valence ionized states of $Fe(CO)_5$ and $CoCp(CO)_2$ were calculated by the SAC-CI method, in which the wave function can be written as[13,14]

$$\Psi_{\text{SAC-CI}} = \sum_K d_K R_K^\dagger \Psi_{\text{SAC}}, \tag{2}$$

where $R_K^\dagger$ represents a symmetry-adapted ionization operator whose coefficient is d_K. The SAC wave function for the neutral ground state is described by the cluster-expansion formalism,

$$\Psi_{\text{SAC}} = \exp\left(\sum_I c_I S_I^\dagger\right)\Phi_0, \tag{3}$$

for the closed-shell Hartree–Fock Φ_0. Singles (S_1) and doubles (S_2) are included for the cluster operator $\{S_I^\dagger\}$

$$S_1 = \sum_i^{\text{occ}} \sum_a^{\text{vac}} (a_{a\alpha}^\dagger a_{i\alpha} + a_{a\beta}^\dagger a_{i\beta})/\sqrt{2}, \tag{4}$$

and

$$S_2 = \sum_{ij}^{\text{occ}} \sum_{ab}^{\text{vac}} (a_{a\alpha}^\dagger a_{i\alpha} + a_{a\beta}^\dagger a_{i\beta})(a_{b\alpha}^\dagger a_{j\alpha} + a_{b\beta}^\dagger a_{j\beta})/2, \tag{5}$$

where $a_{p\omega}$ and $a_{p\omega}^\dagger$ are electron annihilation and creation operators, respectively, for orbital p; $\omega=\alpha$ or β denotes electron spin. The SAC/SAC-CI calculations were carried out with the direct SAC-CI algorithm[19] in which the σ-vector is directly calculated from molecular orbital (MO) integrals without using a cutoff for unlinked (product) terms. In particular, the present calculations included the unlinked terms of S_1 operators such as $S_1 S|\Phi_0\rangle$ and $S_1 R|\Phi_0\rangle$, in addition to the default term.[29] The additional terms were found to be important for describing the electronic structures of transition metal compounds because the weights of some S_1 are large.[21] The details of the SAC-CI computation for this specific case are given in Ref. 21. The SAC/SAC-CI calculations were executed by the GAUSSIAN development version.[30]

Flexible basis sets were used for the SAC/SAC-CI calculations. Ahlrichs' TZV basis[31] was adopted for Fe and Co with augmented p- and f-type functions. The augmented p-type functions (exponents α=0.233 and 0.0823 for Fe and α=0.256 and 0.0973 for Co) were generated by extrapolation of the TZV functions. The exponents off-type functions (α=1.213, 0.3652 for Fe and α=1.341, 0.4004 for Co) were taken from the d-type functions. For C and O, the TZV bases[31] with two d-type polarization functions were used. The polarization functions (α=1.097 and 0.318 for C and α=2.314 and 0.645 for O) were taken from the cc-pVTZ basis.[32] For H, the D95 basis[33] was used with the p-type polarization function α=1.0.

The molecular geometry was optimized by the coupled-cluster singles and doubles (CCSD) method and the metal-ligand bond lengths were refined by the CCSD with perturbative triples [CCSD(T)] method. Because T_1 amplitudes are significant for the CCSD calculations, correction from triples is necessary to obtain accurate metal-ligand bond lengths.[34,35] For the geometry optimization, LANL2DZ (Ref. 36) and D95(d,p) bases[33] were used. The LANL2DZ basis was augmented by adding one d- and f-type function; the exponents were α(d)=α(f)=0.9628 for Fe and α(d)=α(f)=1.066 for Co. These exponents were taken from the original LANL2DZ sets. $Fe(CO)_5$ has D_{3h} point group symmetry and $CoCp(CO)_2$ has C_s symmetry. The geometry parameters determined by the CCSD and CCSD(T) calculations are summarized in Table I.

TABLE I. Bond lengths and bond angles for the SAC-CI calculations (angstroms and degrees).

$Fe(CO)_5$ (D_{3h})		$CoCp(CO)_2$ (C_s)	
Axial CO		CO	
Fe–C	1.805	Co–C	1.749
C–O	1.163	C–O	1.169
Equatorial CO		∠C–Co–C	93.5
Fe–C	1.796	∠Co–C–O	179.3
C–O	1.163	Cp	
		Co–C (average)	2.082
		C–C (average)	1.435
		C–H (average)	1.088
		∠C–C–C (average)	108.0

The 1s electrons of the C and O atoms and the Ar core electrons of metals were excluded from the SAC/SAC-CI calculations. The perturbation-selection technique[20] was used for the SAC/SAC-CI calculation; the thresholds for the ground and ionized states were set to $\lambda_g=\lambda_e$=1.0E−8. The SAC-CI SD-R [singles and doubles R-operator, the R-operators are given in Eqs. (2), (6), and (7)] secular equations were solved using Davidson's iterative method[37] with one-hole (1h, R_1) and two-hole-one-particle (2h1p, R_2) operators for $\{R_I^\dagger\}$

$$R_1 = \sum_i^{\text{occ}} a_{i\alpha}, \tag{6}$$

and

$$R_2 = \sum_{ij}^{\text{occ}} \sum_a^{\text{vac}} a_{j\beta}(a_{a\alpha}^\dagger a_{i\alpha} + a_{a\beta}^\dagger a_{i\beta}). \tag{7}$$

Because we are interested in the interpretation and assignment of PIES spectra, we concentrated on the 1h states and did not examine the shake-up states in detail for which 2h1p configurations are dominant. The SAC-CI SD-R method is less reliable for shake-up states, but it is sufficient to examine the possibility of the existence of low-lying shake-up bands. The relation between the SAC-CI and propagator theory have been discussed in Ref. 38. The ionization cross sections were calculated by the monopole approximation[39] to estimate the relative intensities. For convenience of comparison with experimental spectra, the SAC-CI results were convoluted with a GAUSSIAN envelope whose FWHM was set to 0.2 eV.

Interaction potentials between the target molecule and a ground-state lithium atom were calculated as an approximated potential of target molecule and $He^*(2\,^3S)$ based on the similarity between $He^*(2\,^3S)$ and $Li(2\,^2S)$.[40,41] This approximation enables us to circumvent calculations of highly

TABLE II. IE and character of ionized states for $Fe(CO)_5$.

	KT[b]			SAC-CI				Expt.		
State[a]	IE (eV)	Orbital character[c]	$\langle r^2\rangle$ [d]	IE (eV)	Main cfs (coefficient)[e]	$\lvert R_2\rvert_{max}$ [f]	I[g]	IE (eV)	m [h]	Band
$1\ ^2E'$	9.77	$Fe(3d)+CO(2\pi)+Fe(4p)$	9.57	8.22	$10e'^{-1}(0.94)$	0.13	0.43	8.53	−0.13	1
$1\ ^2E''$	13.37	$Fe(3d)+CO(2\pi)$	7.74	9.69	$3e''^{-1}(0.92)$	0.14	0.43	9.80	−0.08	2
$(^2E'')$				20.18	$10e'^{-1}15a_1'^{+1}3e''^{-1}(0.32)$	0.32	0.002			
$1\ ^2A_2''$	16.40	$CO_a(5\sigma^+)+CO_e(1\pi)$	23.91	14.47	$8a_2''^{-1}(0.93)$	0.06	0.41	14.09	+0.21	3
$2\ ^2E'$	17.07	$CO_e(5\sigma^+)+CO_{e,a}(1\pi)$	22.59	14.72	$9e'^{-1}(0.82)-8e'^{-1}(0.32)+7e'^{-1}(0.30)$	0.06	0.40	14.62	+0.09	4
$1\ ^2A_1'$	16.81	$CO_e(5\sigma^+)-CO_a(5\sigma^+)$	11.64	15.02	$13a_1'^{-1}(0.93)$	0.09	0.41			
$1\ ^2A_2'$	17.25	$CO_e(1\pi)$	28.67	15.24	$1a_2'^{-1}(0.93)$	0.12	0.39			
$2\ ^2E''$	17.06	$CO_e(1\pi)-CO_a(1\pi)$	28.54	15.31	$2e''^{-1}(0.93)$	0.08	0.40	15.41	+0.12	5
$3\ ^2E'$	17.64	$CO_e(5\sigma^+)+CO_{e,a}(1\pi)$	24.78	15.42	$8e'^{-1}(0.84)+9e'^{-1}(0.37)$	0.13	0.39			
$(^2E')$				21.19	$10e'^{-1}12e'^{+1}10e'^{-1}(0.62)+10e'^{-1}12e'^{+1}10e'^{-1}(0.41)$ $+10e'^{-1}11e'^{+1}10e'^{-1}(0.38)$	0.62	0.003			
$2\ ^2A_2''$	18.32	$CO_a(5\sigma^+)+CO_e(1\pi)$	19.60	16.14	$7a_2''^{-1}(0.92)$	0.07	0.40			
$4\ ^2E'$	18.23	$CO_e(5\sigma^+)+CO_a(1\pi)$	22.23	16.22	$7e'^{-1}(0.88)$	0.08	0.40	16.34	+0.08	6
$3\ ^2E''$	18.30	$CO_e(1\pi)+CO_a(1\pi)$	24.38	16.35	$1e''^{-1}(0.93)$	0.07	0.40			
$2\ ^2A_1'$	20.00	$CO_e(5\sigma^+)+CO_a(5\sigma^+)$	26.01	17.02	$12a_1'^{-1}(0.93)$	0.04	0.39			
$5\ ^2E'$	22.08	$CO_e(4\sigma^+)$	29.84	18.59	$6e'^{-1}(0.92)$	0.07	0.37	17.99	0.00	7
$(^2E')$				18.46	$10e'^{-1}15a_1'^{+1}10e'^{-1}(0.48)+10e'^{-1}16a_1'^{+1}10e'^{-1}(0.43)$	0.48	0.001			
$3\ ^2A_1'$	22.03	$CO_e(4\sigma^+)-CO_a(4\sigma^+)$	32.07	18.62	$11a_1'^{-1}(0.92)$	0.08	0.37			
$(^2A_1')$				18.89	$10e'^{-1}15a_1'^{+1}10e'^{-1}(0.47)+10e'^{-1}16a_1'^{+1}10e'^{-1}(0.42)$	0.47	0.006			
$3\ ^2A_2''$	22.59	$CO_a(4\sigma^+)$	30.47	19.22	$6a_2''^{-1}(0.93)$	0.05	0.38			
$4\ ^2A_1'$	23.83	$CO_e(4\sigma^+)+CO_a(4\sigma^+)$	19.05	20.11	$10a_1'^{-1}(0.90)$	0.08	0.36			

[a]The representation of satellite states is given in parentheses.
[b]Koopmans' theorem.
[c]The subscript e and a denote axial and equatorial CO, respectively.
[d]Second moment of ionizing orbital in $(bohr)^2$.
[e]SAC-CI main configurations with the absolute value of coefficient are larger than 0.3.
[f]The maximum absolute value of coefficient for R_2 (1h2p) configurations.
[g]The monopole intensity.
[h]Slope parameter of CEDPICS.

excited states, which involve much greater difficulties than the ground-state calculations. The interaction potential was calculated by the unrestricted CCSD method with 6-311G** basis sets.[42–44] The 6-311G basis is subject to rather severe basis set superposition error.[45] One has to carefully consider it for qualitative analysis of the interaction potential. In this study, we discuss only the qualitative tendency of the slope of CEDPICS, which depends on clearly attractive or repulsive interactions. Therefore, the present level of calculation would be sufficient to obtain the outlook of the interaction potentials. The internal coordinate of the target molecule was fixed to the CCSD/6-311G** optimized geometry of the isolated molecule and the metal-Li distance was changed to calculate the interaction potential. Anisotropy of the interaction potential was studied by the calculation of several coordinates for He^* approaching the metal center from various directions.

IV. RESULTS AND DISCUSSIONS

A. $Fe(CO)_5$

The SAC-CI results for $Fe(CO)_5$ are summarized in Table II with the UPS and 2D-PIES values observed in the present work and the IEs obtained by Koopmans' theorem. We considered that the maxima in the experimental spectra correspond to vertical ionization processes at equilibrium geometry. The effects of molecular vibration were not taken into consideration; the difference may be around a few tenths of an eV.[46] The MOs that are relevant in the outer-valence region of $Fe(CO)_5$ are Fe $(3d)$ and CO[$4\sigma^+$(antibonding), 1π(bonding), $5\sigma^+$(nonbonding), and 2π(antibonding unoccupied)].

For neutral $Fe(CO)_5$, the single-reference SAC with singles and doubles (SD) wave function includes some important singles (S_1) with large amplitudes (in parentheses): $3e''\rightarrow 4e''$ (0.17), $13a_1'\rightarrow 15a_1'$ (0.14), and $1e''\rightarrow 4e''$ (0.10). They are orbital replacement to metal-ligand antibonding MOs; they describe orbital relaxation induced by electron correlation mainly included by S_2 in the SAC expansion. In general, single-reference SAC SD is not a good approximation for this kind of system with large S_1 amplitude.[34] However, the SAC/SAC-CI calculations for IEs are still valid because certain errors can cancel each other in the neutral and ionized states.

The SAC-CI spectrum of $Fe(CO)_5$ is shown in Fig. 1 with the UPS and PIES experimental spectra. From the experiment, seven bands are identified in the outer-valence region below 20 eV and the spectra can be categorized into three regions: region A at 8–10 eV contains bands 1 and 2, region B at 14–17 eV consists of bands 3–6, and region C at 17–20 eV contains band 7. The intensities in the PIES spectra are very different between the regions A–C; the intensi-

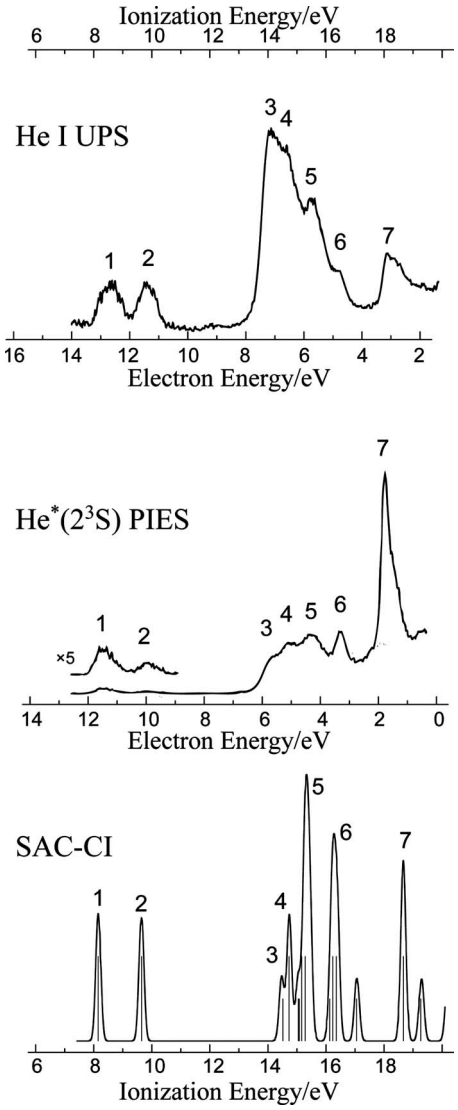

FIG. 1. Observed and calculated ionization spectra for $Fe(CO)_5$.

ties of the bands in region A are very weak, the intensities of the bands in region B are relatively large and band 7 in region C has an extremely large intensity.

This significant difference in PIES intensities is helpful in assigning the ionization character of bands because Penning ionization probability depends on the spatial extent of the density distribution of the ionizing electron. In the framework of MO theory, relative PIES band intensities can be explained by the exterior electron density (EED), defined by the integration of an MO $\phi(\mathbf{r})$ for the exterior region Ω as[6–8]

$$(\mathrm{EED}) = \int_{\Omega} |\phi(\mathbf{r})|^2 \mathrm{d}\mathbf{r}, \tag{8}$$

where Ω is taken over the boundary repulsive molecular surface from which A^* cannot penetrate into the inside. In this study, we will discuss relative PIES intensities using the second moment of MO $\langle r^2 \rangle$ as a rough estimation of the spatial extension of the ionizing MO; this is a rather simpler quantity than EED but is sufficient for qualitative discussion. The second moments of the ionizing MO are given in Table II

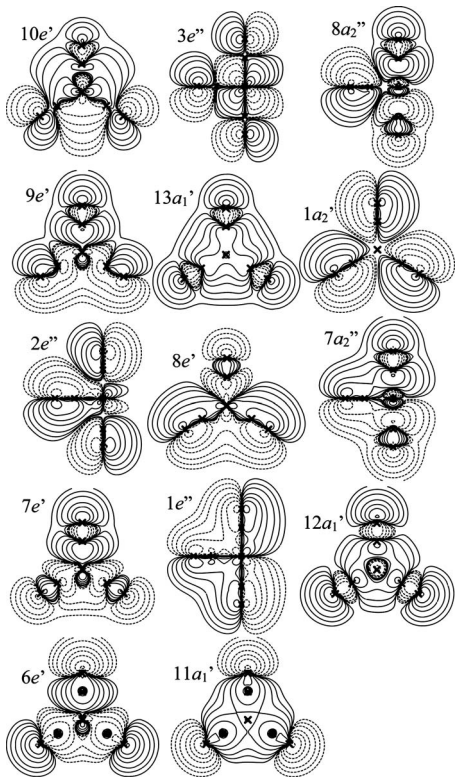

FIG. 2. Valence MO contour plots for $Fe(CO)_5$.

and the contour plots of valence MOs are shown in Fig. 2. For e', a_1', and a_2' orbitals, the plot projected on the σ_h plane is shown and for e'' and a_2'' orbitals, the projection on the σ_v plane is given because they have a nodal plane on σ_h.

The lowest two bands observed by experiment in region A are clearly assigned to $1\ ^2E'$ and $1\ ^2E''$ states. The deviation between the SAC-CI result and experimental IEs was less than 0.3 eV. They are characterized as ionization from the Fe $(3d)$ orbital including back-donation to $CO(2\pi)$. This is consistent with the observed very weak intensity in the PIES spectrum. These orbitals are spatially compact and surrounded by carbonyl groups; therefore, the Penning ionization probability because of collision with He^* must be very small. The contribution of R_2 (2h1p configuration) was also important; the maximum coefficient of R_2 was larger than 0.1. In the SAC-CI method, these ionization operators act on the correlated SAC wave function. Thus, configurations higher than 2h1p are effectively included as unlinked terms, the product of operators such as RS. The difference between the Koopmans' theorem and SAC-CI results is significant because both correlation and relaxation effects are important for this molecule. The SAC-CI method did not shift the Koopmans' IE for these states by a constant amount; the shifts were 1.55 and 3.68 eV for the $1\ ^2E'$ and $1\ ^2E''$ states, respectively.

The different contributions from electron correlation for the $1\ ^2E'$ and $1\ ^2E''$ states can be explained by the molecular symmetry, which is also regarded as the difference in the character of the Fe–CO bonds. Both states were characterized as the ionization of an $Fe(3d)+CO(2\pi)$ electron. By Mulliken population analysis, the contribution from the Fe atomic orbital (AO) to $10e'$ and $3e''$ MOs was 77%. In the

$10e'$ MO the contribution from the Fe p-AOs, which correspond to the $4p$ AO was 25% and that from the Fe $(3d)$ AOs was 52%. In contrast, Fe p-AOs are not mixed into the $3e''$ MO because of its symmetry. Therefore, the $3e''$ MO has a relatively large $3d$-electron character, in which electron correlation is more significant than that for a diffuse $4p$ electron. σ-Donation does not contribute to the $3e''$ MO within a simple orbital level; however, this description is significantly changed by electron correlation.

In region B, four bands were identified by UPS and PIES. In this region, ten states were calculated by the SAC-CI method. The assignment for this region is not obvious because there are dense ionized states and molecular vibration that affects the overlap of bands. Band 3, observed at 14.09 eV, is assigned to the $1\ ^2A_2''$ state. The SAC-CI calculation overestimates the IE by 0.38 eV for this state. Band 4, observed at 14.62 eV, is attributed to the $2\ ^2E'$ state calculated at 14.72 eV. Band 5, observed at 15.41 eV, is assigned to the $2\ ^2E'$ and $3\ ^2E'$ states calculated at 15.31 and 15.42 eV, respectively. Band 6, experimentally observed at 16.34 eV, is assigned to the $2\ ^2A_2''$, $4\ ^2E'$, and $3\ ^2E''$ states calculated in the region 16.14–16.35 eV. For these assignments, the agreement of IEs for bands 4–6 was excellent between the SAC-CI calculation and experiment, but the He I UPS intensities were not well reproduced by the monopole approximation. These bands relate to the symmetry-adapted combinations of $CO(5\sigma^+)$ and $CO(1\pi)$.

The PIES intensities in region B are moderately large. This is consistent with the orbital character of the calculations, which has a relatively large second moment of around 25 $(\text{bohr})^2$. The maximum coefficient of R_2 was around 0.1 or less in this region. This means one-electron ionization character is dominant for these states. However, Koopmans' approximation was still inadequate because important electron correlation and relaxation effects were included in the neutral SAC wave function and they were transferred to ionized states through unlinked terms. Indeed, the energy sequence of ionized states of $2\ ^2E'$ to $2\ ^2E''$ was different between the SAC-CI and Koopmans' theorem predictions.

In region C, band 7 was identified at 17.99 eV with very strong PIES intensity. This band is attributed to the $5\ ^2E'$ and $3\ ^2A_1'$ states, although the calculated IE was higher by 0.6 eV than the experimental value. The SAC-CI calculation suggests another peak for the $2\ ^2A_1'$ state at 17.02 eV. However, the corresponding band was not clearly identified by experiment. The $2\ ^2A_1'$ and $5\ ^2E'$ states have different characters. The $2\ ^2A_1'$ state is due to ionization of the $CO(5\sigma^+)$ electron; thus, it would have a PIES intensity as strong as those in region B. The observed PIES intensity of band 7 is much stronger than those in region B. This strongly suggests a difference in ionization character between regions B and C. Thus, we have assigned band 7 to the $5\ ^2E'$ and $3\ ^2A_1'$ states, which have the ionization character of the $CO(4\sigma^+)$ electrons. The $CO(4\sigma^+)$ orbital has larger amplitude around the oxygen atom than that of the $CO(5\sigma^+)$ orbital, which corresponds to the carbon nonbonding orbital, and therefore the Penning ionization probabilities of $CO(4\sigma^+)$ electrons in $Fe(CO)_5$ are larger than those of the $CO(5\sigma^+)$ electrons. The $2\ ^2A_1'$ state may be covered by the shoulder of band 6 or shake-up satellite peaks which could appear around this energy region. The monopole approximation used in the present study is inadequate for the comparison with the observed intensity of UPS. Furthermore, the Franck–Condon overlap integrals must be taken into account, to discuss the shape of spectrum. The higher-order correlation and relaxation are the possible effects that may shift the peak position and affect to the shape of spectrum. The scalar relativistic and spin-orbit effects would be negligible because the ionizations from carbonyls, which consist of light elements, are dominant in this region.

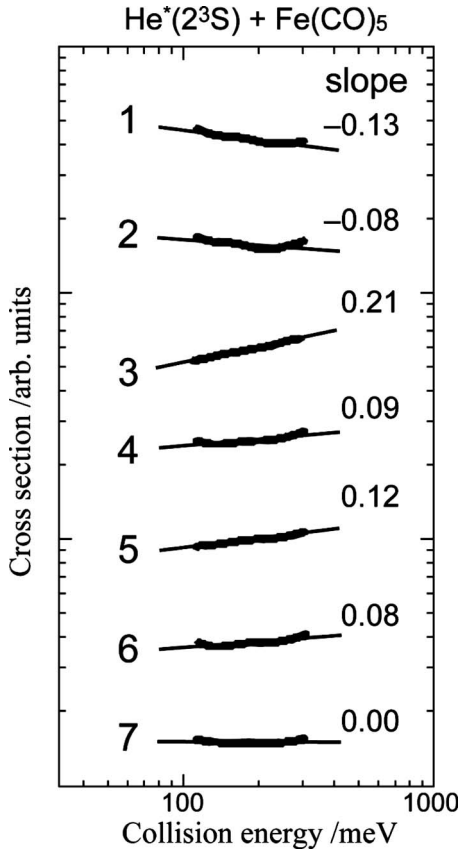

FIG. 3. Collision-energy dependence of Penning ionization cross section for He^*+Fe(CO)5.

The observed CEDPICS of bands 1–7 are shown in Fig. 3 and their slopes are given in Fig. 3 and Table II. The slope is negative for bands 1 and 2, positive for bands 3–6, and zero for band 7. This variation in the slope suggests the different ionization characters between regions A–C because the Penning ionization process crucially depends on the local characteristics of the distributions of the ionizing electron and the slope of CEDPICS is related to the nature of the molecular surface. The relation between the slope of CEDPICS and the nature of the molecular surface has been studied for various molecules[6–8,23] and it is summarized in the following points. A negative slope reflects attractive potentials between a target molecule and He^*. A positive slope reflects repulsive potentials. A steep positive slope suggests a soft molecular surface where the repulsive wall is less steep and a gradual positive slope suggests a hard molecular surface.[7,9] For $Fe(CO)_5$ and He^* the interaction is anisotropic and the slope of CEDPICS reflects the anisotropy. To inter-

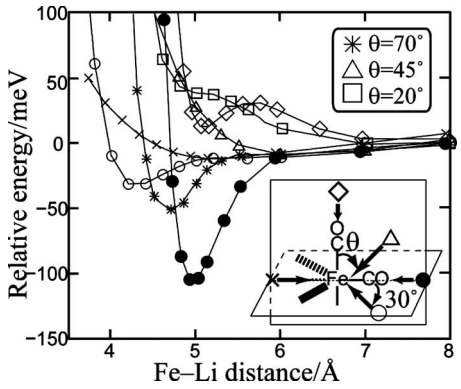

FIG. 4. Potential energy curves for interaction between $Fe(CO)_5$ and Li, θ=0° for axial CO.

pret the CEDPICS, we calculated the interaction potential of $Fe(CO)_5$ and Li, which is regarded as an approximation for the $Fe(CO)_5$–He^* interaction potential. The potential energy curves are shown in Fig. 4. The characteristic interaction has been calculated; the interaction is attractive for the equatorial CO around the Fe–C–O direction, while the interaction in the axial CO direction is basically repulsive. Because the interaction potential is anisotropic and the Penning ionization processes critically depend on the local characteristics of the electron distribution of the ionizing MO, the shape of the MO is relevant to the CEDPICS. The anisotropic interaction of CH_3CN was studied by 2D-PIES, in which attractive and repulsive sites of molecular surface exist.[23]

The slope of CEDPICS for band 1 is more negative than that for band 2; bands 4, 6, and 7 have relatively small slopes of CEDPICS (less than 0.1). By the present calculation, the states that correlate with bands 1, 4, 6, and 7 have E′ representation. The other bands, 2, 3, and 5 have E″, A_2'', and E″ representation, respectively. This indicates that the symmetry with respect to the σ_h plane, which includes equatorial carbonyls, affects the interaction potential between $Fe(CO)_5$ and He^*, and therefore, the slope of CEDPICS.

The relative value of the slope of CEDPICS can be explained by the anisotropic interaction and molecular symmetry. The ionizing orbital in the e' representation has spatial extent in the direction of the equatorial CO. The interaction around the equatorial Fe–C–O direction is attractive for an approaching He^*. An attractive interaction makes the slope of CEDPICS negative. Therefore, bands 1, 4, 6, and 7 have negative or relatively small slopes in CEDPICS. The interaction in the direction of the axial CO is repulsive and the interaction in this direction results in the positive slope of CEDPICS for bands 2, 3, and 5. The ionizing orbital of the E″ and A_2'' states has a nodal plane including the equatorial CO; the interaction around this plane does not affect the slope of CEDPICS. Because we did not obtain a global interaction surface in the present study, we cannot discuss the absolute value of the CEDPICS. However, trends can be qualitatively explained. The SAC-CI calculation and the present assignments are consistent with the experimental finding not only for the IEs but also for the slope of CEDPICS.

B. $CoCp(CO)_2$

The results for $CoCp(CO)_2$ are summarized in Table III; theoretical results by Koopmans' theorem and the SAC-CI method, as well as the experimental results[12] are shown. The MOs of an isolated cyclopentadienyl anion in D_{5h} symmetry are $1a_1'(C1s)$, $1e_1'(C1s)$, $1e_2'(C1s)$, $2a'(\sigma)$, $2e_1'(\sigma)$, $2e_2'(\sigma)$, $3a_1'(\sigma_{CH})$, $3e_1'(\sigma_{CC}^*)$, $3e_2'(\sigma_{CC}^*)$, $1a_2''(\pi)$, and $1e_1''(\pi)$. For neutral $CoCp(CO)_2$, the important S_1 in the SAC wave function with coefficients larger than 0.1 are $16a''\rightarrow18a''$ (0.15), $17a''\rightarrow23a''$ (0.14), $17a''\rightarrow24a''$ (−0.13), $25a'\rightarrow30a'$ (0.11), and $17a''\rightarrow27a''$ (−0.11); they mainly have the character of metal-ligand orbital rearrangement because of electron correlation.

The SAC-CI spectrum is compared to the UPS and PIES experimental spectra in Fig. 5. In the previous work,[12] 17 states were identified for UPS and PIES in the energy range below 20 eV based on the theoretical calculations. However, the number of calculated states seemed to be small because $CoCp(CO)_2$ has 22 outer-valence orbitals.[26] The present calculation shows that the spectrum below 20 eV consists of the expected 22 states, for which bands 8 and 9, 10–15, 16 and 17, and 18–22 were not clearly resolved by the experiment. In this work, we will discuss the bands numbered by 1–22. In the 7–11 eV region, six bands were identified with small PIES intensities. In the 13–16 eV region, bands 7–17 were suggested but bands in this region were overlapping and clear identification was impossible; the PIES intensities in this region were moderate. In the 17–19 eV region, bands 18–22 were suggested. A very strong band assigned as 18 and 19 was observed by PIES; the shoulder was assumed to be bands 20–22. It was difficult to assign the experimental spectra with the previous SAC-CI calculation;[12] therefore, we will discuss the assignment of the spectra based on the improved calculation in this study.

In the 7–8 eV region, two overlapping bands 1 and 2 were suggested by the experiment. For these bands, two $^2A'$ states are calculated at 7.03 and 7.14 eV by the SAC-CI method. Band 3, observed at 8.54 eV, is calculated at 7.94 eV. In the 9–11 eV region three overlapping bands were identified by the experiment: band 4 at 9.35 eV, band 5 at 10.00 eV, and band 6 as the shoulder of band 5, at 10.49 eV. The calculated SAC-CI IEs are 9.18, 9.46, and 9.51 eV, respectively. The SAC-CI calculation reproduced well the relative band positions from the first IE but the absolute values were underestimated by about 0.5 eV. This error would come from the multireference character of the ground state as shown by the magnitude of the S_1 amplitude.

We discuss the orbital character of these states based on Koopmans' theorem to interpret the effect of electron correlations and orbital relaxation. The lowest state has the character of ionization from the $28a'$ highest occupied molecular orbital (HOMO), which is a bonding orbital between the $1e_1''$ π orbital of Cp and 2π orbitals of two carbonyls. This orbital also has Co $(3d)$ character through back-donation from Co $(3d)$ to CO(2π); the percentage of Co AOs in the gross orbital population was 24%. The next two states, $2\ ^2A'$ and $1\ ^2A''$ have the character of ionization from Co $(3d)$. The contribution from AOs of Co to the $27a'$ and $16a''$ orbitals is

TABLE III. IEs and character of ionized states for $CoCp(CO)_2$.

	KT[b]			SAC-CI					Expt.[c]		
State[a]	IE (eV)	Orbital character[d]	$\langle r^2\rangle$ [e]	IE (eV)	Main cfs (coef.)[f]	$\lvert R_2\rvert_{max}$ [g]	I[h]	IE (eV)	m [i]	Band
$1\ ^2A'$	8.10	$Cp(1e_1'')+CO(2\pi)^+$	15.81	7.03	$28a'^{-1}(0.82)+26a'^{-1}(0.45)$	0.09	0.46	7.59	−0.42	1
$2\ ^2A'$	11.70	Co $(3d)$	5.47	7.14	$27a'^{-1}(0.79)+26a'^{-1}(0.34)$	0.13	0.45	7.94	−0.47	2
(A')				18.33	$27a'^{-1}23a''^{+1}17a''^{-1}(0.29)$ [j]	0.29	0.007			
$1\ ^2A''$	12.38	Co $(3d)$	4.68	7.94	$16a''^{-1}(0.89)$	0.15	0.45	8.54	−0.29	3
(A'')				18.76	$17a''^{-1}23a''^{+1}16a''^{-1}(0.31)$	0.31	0.004			
$3\ ^2A'$	13.83	$Co(3d)+CO(2\pi)^+$	10.51	9.18	$25a'^{-1}(0.74)+24a'^{-1}(0.37)$	0.12	0.45	9.35	−0.20	4
(A')				19.42	$17a''^{-1}23a''^{+1}25a'^{-1}(0.34)-17a''^{-1}24a''^{+1}25a'^{-1}(0.31)$	0.34	0.004			
$2\ ^2A''$	9.55	$Cp(1e_1'')$	16.33	9.46	$17a''^{-1}(0.95)$	0.09	0.44	10.00	−0.34	5
(A'')				19.37	$28a'^{-1}20a''^{+1}28a'^{-1}(0.48)$	0.48	0.002			
(A'')				19.74	$28a'^{-1}20a''^{+1}28a'^{-1}(0.49)$	0.49	0.001			
$4\ ^2A'$	11.72	$Co(3d)+Cp(1e_1'')$	7.51	9.51	$26a'^{-1}(0.72)-28a'^{-1}(0.45)-27a'^{-1}(0.40)$	0.08	0.43	10.49	−0.32	6
(A')				16.95	$28a'^{-1}23a''^{+1}17a''^{-1}(0.32)-16a''^{-1}23a''^{+1}28a'^{-1}(0.32)$	0.32	0.004			
(A')				18.08	$17a''^{-1}23a''^{+1}28a'^{-1}(0.25)$ [j]	0.25	0.004			
(A')				18.46	$28a'^{-1}29a'^{+1}28a'^{-1}(0.80)$	0.80	0.006			
$5\ ^2A'$	14.45	$Cp(1a_2'')$	15.03	12.64	$24a'^{-1}(0.71)-25a'^{-1}(0.48)+23a'^{-1}(0.37)$	0.10	0.40	13.0	−0.23	7
(A')				19.63	$28a'^{-1}32a'^{+1}28a'^{-1}(0.59)-28a'^{-1}30a'^{+1}28a'^{-1}(0.59)$	0.59	0.003			
$3\ ^2A''$	14.61	$Cp(3e_2')$	19.01	12.86	$15a''^{-1}(0.94)$	0.10	0.41	13.3	−0.17	8.9
$6\ ^2A'$	14.68	$Cp(3e_2')$	16.92	12.87	$23a'^{-1}(0.81)-24a'^{-1}(0.48)$	0.09	0.41			
$4\ ^2A''$	15.15	$Cp(3e_1')$	20.45	13.35	$14a''^{-1}(0.94)$	0.08	0.40	13.5∼		10–15
$7\ ^2A'$	15.73	$Cp(3e_1')$	20.63	13.74	$22a'^{-1}(0.94)$	0.11	0.40	(14.4)	−0.28	
$5\ ^2A''$	16.43	$CO(5\sigma)^-+CO(2\pi)^-$	22.56	14.50	$13a''^{-1}(0.89)$	0.08	0.43			
$6\ ^2A''$	17.08	$CO(1\pi)^-$	28.20	15.00	$12a''^{-1}(0.91)$	0.17	0.41			
(A'')				14.94	$28a'^{-1}23a''^{+1}28a'^{-1}(0.44)-28a'^{-1}24a''^{+1}28a'^{-1}(0.39)$ $-28a'^{-1}27a''^{+1}28a'^{-1}(0.34)$	0.44	0.002			
$7\ ^2A''$	17.09	$CO(1\pi)^-$	21.39	15.11	$11a''^{-1}(0.88)$	0.12	0.42			
$8\ ^2A'$	17.24	$CO(1\pi)^+$	27.85	15.14	$21a'^{-1}(0.93)$	0.17	0.41	15.5	−0.43	16,17
$9\ ^2A'$	17.36	$CO(1\pi)^+$	25.24	15.31	$20a'^{-1}(0.88)$	0.12	0.41			
$10\ ^2A'$	18.72	$CO(5\sigma)^+$	20.27	15.84	$19a'^{-1}(0.64)+28a'^{-1}23a''^{+1}16a''^{-1}(0.40)$ $-28a'^{-1}24a''^{+1}16a''^{-1}(0.37)-28a'^{-1}27a''^{+1}16a''^{-1}(0.34)$	0.40	0.22			
(A')				15.93	$19a'^{-1}(0.59)-28a'^{-1}23a''^{+1}16a''^{-1}(0.44)$ $+28a'^{-1}24a''^{+1}16a''^{-1}(0.41)+28a'^{-1}27a''^{+1}16a''^{-1}(0.37)$	0.44	0.19			
$11\ ^2A'$	19.69	$Cp(3a_1')$	20.70	17.03	$18a'^{-1}(0.89)$	0.10	0.33	17.64	−0.26	18,19
(A')				16.96	$16a''^{-1}23a''^{+1}28a'^{-1}(0.41)-16a''^{-1}24a''^{+1}28a'^{-1}(0.37)$ $-16a''^{-1}27a''^{+1}28a'^{-1}(0.34)$	0.41	0.004			
(A')				17.25	$17a''^{-1}23a''^{+1}27a'^{-1}(0.41)+27a'^{-1}23a''^{+1}17a''^{-1}(0.40)$ $-17a''^{-1}24a''^{+1}27a'^{-1}(0.37)$ $-27a'^{-1}24a''^{+1}17a''^{-1}(0.37)-17a''^{-1}27a''^{+1}27a'^{-1}(0.34)$ $-27a'^{-1}27a''^{+1}17a''^{-1}(0.33)$	0.41	0.059			
$8\ ^2A''$	20.43	$Cp(2e_2')$	20.77	17.45	$10a''^{-1}(0.88)$	0.16	0.34			
(A'')				17.81	$16a''^{-1}23a''^{+1}17a''^{-1}(0.53)-16a''^{-1}24a''^{+1}17a''^{-1}(0.48)$ $+17a''^{-1}23a''^{+1}16a''^{-1}(0.46)$ $-16a''^{-1}27a''^{+1}17a''^{-1}(0.44)-17a''^{-1}24a''^{+1}16a''^{-1}(0.42)$ $-17a''^{-1}27a''^{+1}16a''^{-1}(0.39)$	0.53	0.026			
$12\ ^2A'$	20.45	$Cp(2e_2')$	21.04	17.55	$17a'^{-1}(0.88)$	0.14	0.34			
(A')				18.32	$25a'^{-1}23a''^{+1}17a''^{-1}(0.46)-25a'^{-1}24a''^{+1}17a''^{-1}(0.42)$ $-25a'^{-1}27a''^{+1}17a''^{-1}(0.39)$	0.46	0.007			
$9\ ^2A''$	21.72	$CO(4\sigma)^-$	32.25	18.24	$9a''^{-1}(0.88)$	0.11	0.34	18.3(s)		
$13\ ^2A'$	22.37	$CO(4\sigma)^+$	26.01	18.83	$16a'^{-1}(0.91)$	0.12	0.38			

[a]The representation of satellite states is given in parentheses.
[b]Koopmans' theorem.
[c]Reference 12.
[d]The superscript denotes that the two carbonyl orbitals are in-phase (+) or out-of-phase (−).
[e]Second moment of ionizing orbital in $(bohr)^2$.
[f]SAC-CI main configurations with the absolute value of coefficient are larger than 0.3.
[g]The maximum absolute value of coefficient for R_2 (1h2p) configurations.
[h]The monopole intensity.
[i]Slope parameter of CEDPICS.
[j]There are no configurations whose coefficient is larger than 0.3.

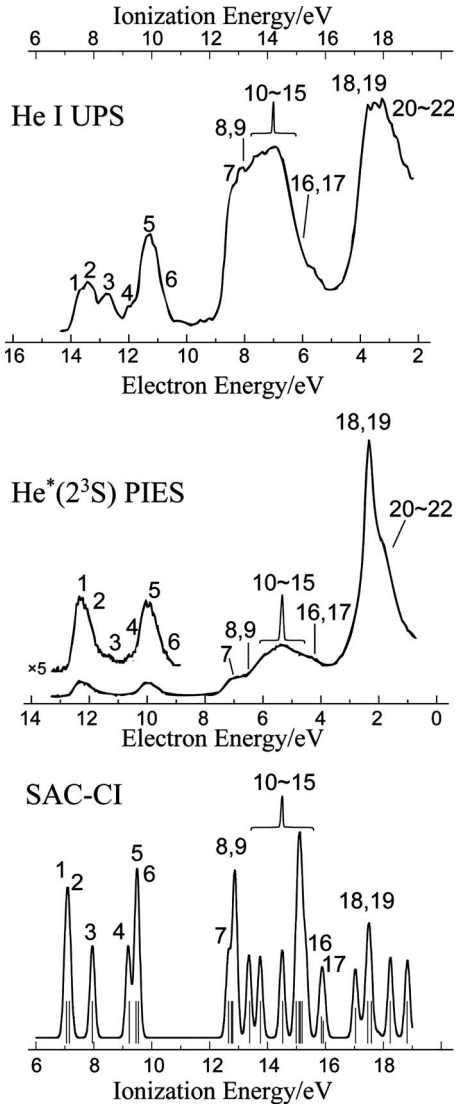

FIG. 5. Observed (Ref. 12) and calculated ionization spectra for $CoCp(CO)_2$.

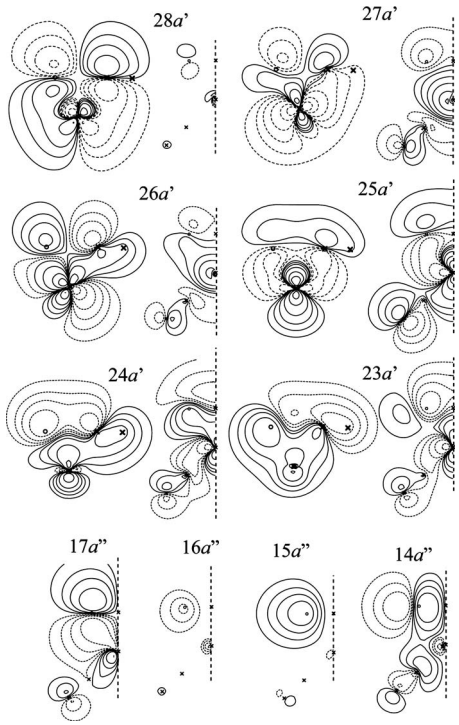

FIG. 6. Valence MO contour plot for $CoCp(CO)_2$.

about 84% by orbital population analysis. The 3 $^2A'$ and 4 $^2A'$ states also have the main character of Co (3*d*) ionization; the contributions from AOs of Co are about 56% and 69%, respectively. The 2 $^2A''$ state has the ionization character of 86% Cp π orbital and the contribution from Co is 12%. The states whose ionization contribution from Co exceeded 50% were 2 $^2A'$, 1 $^2A''$, 3 $^2A'$, and 4 $^2A'$ by Koopmans' theorem.

The weight of Co (3*d*) AOs in the ionizing orbital is correlated with the relaxation of the electronic wave function following ionization, namely, the difference between the SAC-CI and Koopmans' theorem values, which includes the orbital relaxation and electron correlation effects. The relaxations are significant for the 2 $^2A'$, 1 $^2A''$, and 3 $^2A'$ states; the energy shifts are about 4.5 eV. The 2h1p configurations are important for these states and the maximum coefficients are larger than 0.1. For the 1 $^2A'$ and 2 $^2A''$ states, which are mainly ionization of a Cp π-electron, the relaxation is about 1 eV or less. In particular, the shift of the 2 $^2A''$ state was only 0.09 eV. This difference in the relaxation effect, which depends on the orbital character, changed the Koopmans sequence of the ionized states by the SAC-CI method. The HOMO as well as the next-HOMO have Cp π character and the MOs with Co (3*d*) character are deeper by about 2–4 eV than the next HOMO. This energy gap is filled with a large relaxation effect on the Co (3*d*) orbital; the 2 $^2A'$, 1 $^2A''$, and 3 $^2A'$ states have lower IEs than the IE of the 2 $^2A''$ state.

The second moment of the MOs given in Table III can consistently explain the relative intensities of the PIES spectra of bands 1–6 based on this assignment. Bands 1 and 5 have stronger PIES intensity than those of bands 3, 4, and 6. The second, third, fourth, and sixth states have the ionization character of the Co (3*d*) orbital that is surrounded by ligands; therefore, the intensities of these states are small. The contour plots of valence MOs of $CoCp(CO)_2$ are shown in Fig. 6. The plots projected on the σ_h plane and OC–Co–CO plane are displayed for a' orbitals, while, for a'' orbitals, the projection on the OC–Co–CO plane are shown because the orbitals have a σ_h nodal plane. The projections of the a' orbital on the OC–Co–CO plane are symmetric for the σ_h plane and those of a'' are antisymmetric; thus, Fig. 6 shows only one side of the molecule. These plots show the diffuseness of the $28a'$ orbital in comparison with the $27a'$ or $25a'$ orbital. The PIES intensities relate to the orbital extension.

In the 13.0–13.3 eV region, a shoulder and bands 7–9 were observed by UPS and a plateau was obtained in this region by PIES. These bands are assigned to the 5 $^2A'$, 3 $^2A''$, and 6 $^2A'$ states calculated at 12.64, 12.86, and 12.87 eV, respectively. Several overlapping peaks, bands 10–15, were suggested in the 13.5–15 eV region by the experiment. For these peaks, seven 1h states, 4 $^2A''$, 7 $^2A'$, 5 $^2A''$, 6 $^2A''$, 7 $^2A''$, 8 $^2A'$, and 9 $^2A'$, were calculated by the SAC-CI method in the energy range from 13.35 to 15.31 eV. These states have the character of ionization from Cp($3e_1'$),

$CO(5\sigma^+)$, and $CO(1\pi)$ orbitals. The second moment of these orbitals is about 20 $(bohr)^2$, but the $12a'$ MO, the main configuration of the 6 $^2A'$ state at 15.00 eV, has a large second moment of about 28 $(bohr)^2$. This explains the shape of the PIES spectrum in this region, which has a maximum intensity around 14.8 eV.

A shoulder was observed at 15.5 eV by the UPS and PIES experiments. This shoulder would be assigned as the 10 $^2A'$ state. By the SAC-CI calculation, this state was split into two with almost equal intensities by strong interaction with 2h1p configurations; the IEs were 15.84 and 15.93 eV. These states have the character of one-electron ionization from the $CO(5\sigma^+)$ orbital and metal-ligand CT-type excitations.

In the 17–19 eV region, a strong band at 17.64 eV was observed by UPS with a shoulder at 18.3 eV. The band also has strong intensity in PIES. In this region, 11 $^2A'$, 8 $^2A''$, 12 $^2A'$, 9 $^2A''$, and 13 $^2A'$ states were calculated as the main peaks. The lower three states have the character of ionization from $Cp(\sigma)$ orbitals. The second moment of these orbitals was about 20 $(bohr)^2$. The higher states are ionizations from $CO(4\sigma^+)$ orbitals. The spatial extent of these orbitals is larger than that of $Cp(\sigma)$ orbitals. The intensity of the PIES bands in this region cannot be explained solely by the spatial extension of MOs. An EED that explicitly considers the molecular surface is necessary to reflect the anisotropy of the molecular surface. In addition, a simple MO theory may be insufficient to explain even the qualitative trends in this energy region because the 2h1p configurations and other correlation effects may be important in this region. Several shake-up satellite states are calculated to be in the energy region above 18 eV. These states would affect the band shapes in this energy region.

For this molecule, several shake-up satellite states were calculated below 20 eV. There is some possibility that the IEs and intensities of these shake-up states are affected by including triples (3h2p) and higher configurations with the SAC-CI general-*R* method. Although our discussion remains qualitative, we found two low-lying satellites that strongly interact with one-hole states at 14.94 and 15.93 eV. Thus, the classification of these as main and satellite was meaningless. It should be noted that the IEs of shake-up states significantly depend on molecular geometries and the bandwidths of peaks depend on Franck–Condon overlap. Accurate calculations including 3h2p and higher *R* operators are necessary in this energy region for a more reliable discussion.

The CEDPICS obtained by 2D-PIES were reported in our previous study.[12] In this study, we particularly discuss the bands of the higher energy region where our previous calculation was inaccurate. The interaction potentials were calculated for $CoCp(CO)_2$ and Li to discuss the anisotropic interactions; the results are shown in Fig. 7. The interaction is attractive in the direction of Co–C–O and the Cp ring in which θ is less than 20° [the angle of (center of Cp)–Co–C(Cp) is about 35°].

The slopes of CEDPICS are given in Table III. All of the slopes of CEDPICS obtained by the 2D-PIES experiment were negative. This indicates that the interaction is basically attractive or the Penning ionization probability is dominant

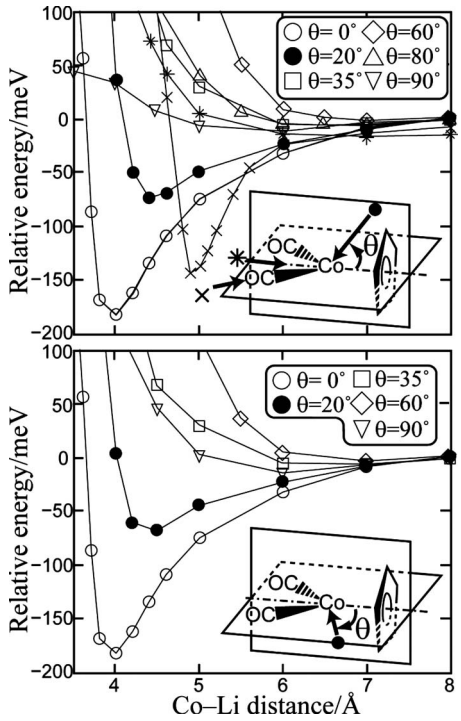

FIG. 7. Potential energy curves for interaction between $CoCp(CO)_2$ and Li, θ=0° for the center of Cp.

in the direction of the attractive potential. The variation of the slope was −0.17 to −0.47; the variation reflects the anisotropic distribution of ionizing electron density. According to our assignment, the states are classified into A′ and A″ representations: bands 1, 2, 4, 6, and 7 are A′ and bands 3, 5, and 8 are A″. Within the A″ state, band 5 has the most negative slope and band 8 has the least negative slope of CEDPICS. This trend can be clearly explained by the orbital distribution of each main configuration. The main configuration of band 5, 2 $^2A''$ state, is ionization from the $17a''$ orbital, which has a large distribution on top of the Cp ring; therefore, attractive interaction affects this state. The main configuration of band 8, 3 $^2A''$ state, is ionization from the $15a''$ orbital, which has a large distribution on the side of the Cp ring; therefore, repulsive interaction reduces the absolute value of the slope of CEDPICS. The relatively small slopes of CEDPICS for bands 4 and 8 in the A′ states can be explained by the larger distribution on the side of the Cp ring in the $25a'$ and $24a'$ orbitals.

The slopes of CEDPICS for bands 10–15, 16–17, and 18–19 were −0.28, −0.43, and −0.26, respectively. These relative slope values could not be well explained in our previous report because their assignment was ambiguous. Based on the assignment of the present calculation, the relation between the CEDPICS and the shapes of ionizing MOs were elucidated for these bands. Bands 10–15 are assigned to ionization from the $14a''$ and $22a'$ MOs; they have the character of the $Cp(3e')$ orbital. Bands 18–19 are assigned to ionization from the $18a'$ MOs, whose character is the $Cp(3a_1')$ orbital. Both have $Cp(\sigma)$ character, which has a distribution on the side of the ring rather than the top of the ring. A repulsive interaction in this direction contributes to the positive slope of CEDPICS; therefore, the observed slopes are

relatively small for these bands. Bands 16–17 have a large negative value for the slope of CEDPICS. This negative slope would result from the $19a'$ MO, which has the character of $CO(5\sigma^+)$ because the interaction potential in the Co–CO direction is strongly attractive. The calculated IE for this state is 15.84 eV, which is consistent with the observation.

V. CONCLUSIONS

The valence ionized states in the energy region up to 20 eV of $Fe(CO)_5$ and $CoCp(CO)_2$ have been studied by UPS, 2D-PIES, and SAC-CI calculations. The SAC-CI results agree well with the experimentally observed IEs. Reliable assignment for valence ionized states of these two molecules were provided based on the SAC-CI calculations that are consistent with the intensities of PIES and the slope of CEDPICS obtained by 2D-PIES. The present study demonstrated a rigorous approach for investigating the valence electronic structures of polyatomic molecules with 2D-PIES and high-level *ab initio* calculations.

For $Fe(CO)_5$, seven bands were identified by UPS and PIES. These states were assigned by the SAC-CI calculations, based on the IEs and ionizing orbital characters; three regions of 8–10, 14–17, and 17–20 eV were attributed to ionizations from the $Fe(d)+CO(2\pi)$, $CO(5\sigma^+)$ and $CO(1\pi)$, and $CO(4\sigma^+)$, respectively. The spatial extent of the ionizing orbitals could consistently explain the intensities observed in PIES. The two states in the 8–10 eV region are the $1\ ^2E'$ and $1\ ^2E''$ states. The electron correlation effect in the $1\ ^2E''$ state is much larger than that in the $1\ ^2E'$ state because of its Fe $(3d)$ character in the MO. Because of molecular symmetry, mixing of the Fe $(4p)$ orbital in the $1\ ^2E''$ state cannot be described at the simple orbital level.

For $CoCp(CO)_2$, 22 bands are assumed below 20 eV from the present theoretical calculations, in contrast to the previous study where only 17 bands were analyzed. The present SAC-CI calculation reproduced these 22 ionized states with good accuracy. For the lower six bands in the 7–11 eV region, the present calculation underestimated IEs by about 0.5 eV, but the relative peak positions were well reproduced. The SAC-CI results explained the relative intensities of the PIES bands for these six bands. Several overlapping bands were observed in the 13–16 eV region; the SAC-CI calculation provided reliable assignments for this region. The present calculation suggested the existence of several shake-up satellites above 15 eV.

The interaction potentials between He^* and target molecules were studied by CCSD/6-311G** using the approximation where He^* was replaced by Li. For $Fe(CO)_5$, attractive interaction was obtained for the equatorial Fe–C–O direction, while the interaction for the axial Fe–C–O direction was repulsive. Ionized states of E'' and A_2'' symmetry have a nodal plane including equatorial carbonyls and therefore the attractive interaction does not affect the CEDPICS for these states. This symmetry analysis explained the relative slopes of CEDPICS. For $CoCp(CO)_2$, an attractive interaction was calculated for the Co–C–O and Co–Cp directions. Based on the present assignment, the large negative slope of CEDPICS for bands 16–17 was explained by the interaction in the Co–C–O direction; this observation had not been clearly explained in the previous study.

ACKNOWLEDGMENTS

The authors acknowledge support from a Grant-in-Aid for Scientific Research from the Japan Society for the Promotion of Science, the Next Generation Supercomputing Project, and the Molecular-Based New Computational Science Program, NINS. The computations were performed using the Research Center for Computational Science, Okazaki, Japan.

[1] T. Koopmans, Physica (Amsterdam) **1**, 104 (1934).
[2] J. C. Green, Acc. Chem. Res. **27**, 131 (1994); E. I. Solomon, L. Basumallick, P. Chen, and P. Kennepohl, Coord. Chem. Rev. **249**, 229 (2005).
[3] M. A. Coplan, J. H. Moor, and J. P. Doering, Rev. Mod. Phys. **66**, 985 (1994).
[4] M. S. Deleuze, W. N. Pang, A. Salam, and R. C. Shang, J. Am. Chem. Soc. **123**, 4049 (2001); S. Knippenberg, K. L. Nixon, H. Mackenzie-Ross, M. J. Brunger, F. Wang, M. S. Deleuze, J. P. Francois, and D. A. Winkler, J. Phys. Chem. A **109**, 9324 (2005).
[5] J. Rolke, Y. Zheng, C. E. Brion, S. J. Chakravorty, E. R. Davidson, and I. E. McCarthy, Chem. Phys. **215**, 191 (1997).
[6] K. Ohno, H. Yamakado, T. Ogawa, and T. Yamata, J. Chem. Phys. **105**, 7536 (1996).
[7] K. Ohno, Bull. Chem. Soc. Jpn. **77**, 887 (2004), and references therein.
[8] N. Kishimoto and K. Ohno, Int. Rev. Phys. Chem. **26**, 93 (2007).
[9] M. Ohno and W. von Niessen, J. Chem. Phys. **95**, 373 (1991).
[10] W. von Niessen and L. S. Cederbaum, Mol. Phys. **43**, 897 (1981); M. Ohno, W. von Niessen, and J. Schule, Chem. Phys. **158**, 1 (1991); J. S. Lin and J. V. Ortiz, Chem. Phys. Lett. **171**, 197 (1990); S. Kambalapalli and J. V. Ortiz, J. Phys. Chem. A **108**, 2988 (2004); M. Pernpointner, T. Rapps, and L. S. Cederbaum, J. Chem. Phys. **129**, 174302 (2008).
[11] S. Knippenberg, J.-P. Francois, and M. S. Deleuze, J. Comput. Chem. **27**, 1703 (2006); T. Horio, T. Hatamoto, S. Maeda, N. Kishimoto, and K. Ohno, J. Chem. Phys. **124**, 104308 (2006); N. Kishimoto, Y. Hagihara, K. Ohno, S. Knippenberg, J.-P. Francois, and M. S. Deleuze, J. Phys. Chem. A **109**, 10535 (2005); F. Morini, B Hajgató, M. S. Deleuze, C. G. Ning, and J. K. Deng, *ibid.* **112**, 9083 (2008); B Hajgató, M. S. Deleuze, and F. Morini, *ibid.* **113**, 7138 (2009).
[12] N. Kishimoto and K. Ohno, J. Phys. Chem. A **113**, 14559 (2009).
[13] H. Nakatsuji and K. Hirao, J. Chem. Phys. **68**, 2053 (1978).
[14] H. Nakatsuji, Chem. Phys. Lett. **59**, 362 (1978); **67**, 329 (1979); **67**, 334 (1979).
[15] O. Kitao and H. Nakatsuji, J. Chem. Phys. **87**, 1169 (1987); J. Wan, M. Ehara, M. Hada, and H. Nakatsuji, *ibid.* **113**, 5245 (2000); J. Wan, M. Hada, M. Ehara, and H. Nakatsuji, *ibid.* **114**, 5117 (2001); H. Nakatsuji, M. Komori, and O. Kitao, Chem. Phys. Lett. **142**, 446 (1987); M. Ehara, M. Nakata, and H. Nakatsuji, Mol. Phys. **104**, 971 (2006).
[16] P. Tomasello, J. Hasegawa, and H. Nakatsuji, Europhys. Lett. **41**, 611 (1998); M. Ehara, Y. Ohtsuka, and H. Nakatsuji, Chem. Phys. **226**, 113 (1998); P. Tomasello, M. Ehara, and H. Nakatsuji, J. Chem. Phys. **118**, 5811 (2003).
[17] M. Ehara, M. Ishida, and H. Nakatsuji, J. Chem. Phys. **117**, 3248 (2002); M. Ehara, Y. Ohtsuka, H. Nakatsuji, M. Takahashi, and Y. Udagawa, *ibid.* **122**, 234319 (2005); M. Ehara, S. Yasuda, and H. Nakatsuji, Z. Phys. Chem. **217**, 161 (2003).
[18] K. Ishimura, M. Hada, and H. Nakatsuji, J. Chem. Phys. **117**, 6533 (2002).
[19] R. Fukuda and H. Nakatsuji, J. Chem. Phys. **128**, 094105 (2008).
[20] H. Nakatsuji, Chem. Phys. **75**, 425 (1983); H. Nakatsuji, J. Hasegawa, and M. Hada, J. Chem. Phys. **104**, 2321 (1996).
[21] R. Fukuda, S. Hayaki, and H. Nakatsuji, J. Chem. Phys. **131**, 174303 (2009).
[22] E. W. Plummer, W. R. Salaneck, and J. S. Miller, Phys. Rev. B **18**, 1673 (1978).
[23] T. Horio, M. Yamazaki, S. Maeda, N. Kishimoto, and K. Ohno, J. Chem. Phys. **123**, 194308 (2005).

[24] Y. Harada, K. Ohno, and H. Mutoh, J. Chem. Phys. **79**, 3251 (1983).
[25] E. J. Baerends, Ch. Oudshoorn, and A. Oskam, J. Electron Spectrosc. Relat. Phenom. **6**, 259 (1975); C. Angeli, G. Berthier, C. Rolando, M. Sablier, C. Alcaraz, and O. Dutuit, J. Phys. Chem. A **101**, 7907 (1997).
[26] X. Li, G. M. Bancroft, R. J. Puddephatt, Y.-F. Hu, and K. H. Tan, Organometallics **15**, 2890 (1996).
[27] K. Kimura, S. Katsumata, Y. Achiba, T. Yamazaki, and S. Iwata, *Handbook of He I Photoelectron Spectra of Fundamental Organic Molecules* (Japan Scientific Societies, Tokyo, 1981).
[28] N. Kishimoto, J. Aizawa, H. Yamakado, and K. Ohno, J. Phys. Chem. A **101**, 5038 (1997).
[29] H. Nakatsuji, M. Hada, M. Ehara, K. Toyota, R. Fukuda, J. Hasegawa, M. Ishida, T. Nakajima, Y. Honda, O. Kitao, and H. Nakai, SAC-CI GUIDE (2005) (PDF file is available at http://www.qcri.or.jp/sacci/).
[30] M. J. Frisch, G. W. Trucks, H. B. Schlegel *et al.*, GAUSSIAN Development Version, Revision H.01 (Gaussian, Inc., Wallingford, CT, 2009).
[31] A. Schäfer, C. Huber, and R. Ahlrichs, J. Chem. Phys. **100**, 5829 (1994).
[32] T. H. Dunning, Jr., J. Chem. Phys. **90**, 1007 (1989).
[33] T. H. Dunning, Jr. and P. J. Hay, in *Modern Theoretical Chemistry*, edited by H. F. Schaefer III (Plenum, New York, 1977), Vol. 3, pp. 1–27.
[34] T. J. Lee and P. R. Taylor, Int. J. Quantum Chem., Symp. **23**, 199 (1989).
[35] O. González-Blanco and V. Branchadell, J. Chem. Phys. **110**, 778 (1999).
[36] P. J. Hay and W. R. Wadt, J. Chem. Phys. **82**, 270 (1985); **82**, 299 (1985); W. R. Wadt and P. J. Hay, *ibid.* **82**, 284 (1985).
[37] E. R. Davidson, J. Comput. Phys. **17**, 87 (1975); K. Hirao and H. Nakatsuji, *ibid.* **45**, 246 (1982).
[38] F. Mertins and J. Schirmer, Phys. Rev. A **53**, 2140 (1996).
[39] S. Süzer, S. T. Lee, and D. A. Shirley, Phys. Rev. A **13**, 1842 (1976); R. I. Martin and D. A. Shirley, J. Chem. Phys. **64**, 3685 (1976).
[40] A. Niehaus, Adv. Chem. Phys. **45**, 399 (1981).
[41] H. Hotop, T. E. Roth, M.-W. Ruf, and A. J. Yencha, Theor. Chem. Acc. **100**, 36 (1998).
[42] R. Krishnan, J. S. Binkley, R. Seeger, and J. A. Pople, J. Chem. Phys. **72**, 650 (1980).
[43] A. J. H. Wachters, J. Chem. Phys. **52**, 1033 (1970); P. J. Hay, *ibid.* **66**, 4377 (1977).
[44] K. Raghavachari and G. W. Trucks, J. Chem. Phys. **91**, 1062 (1989).
[45] D. Moran, A. C. Simmonett, F. E. Leach III, W. D. Allen, P. v. R. Schleyer, and H. F. Schaefer III, J. Am. Chem. Soc. **128**, 9342 (2006).
[46] L. S. Cederbaum and W. Domcke, J. Chem. Phys. **64**, 603 (1976); E. R. Davidson and A. A. Jarzęcki, Chem. Phys. Lett. **285**, 155 (1998); L. S. Cederbaum, W. Domcke, J. Schirmer, and W. von Niessen, Adv. Chem. Phys. **65**, 115 (1986); A. D. O. Bawagan and E. R. Davidson, *ibid.* **110**, 215 (1999).